CILAMCE 2017
Florianópolis - Santa Catarina - Brazil

ON THE LOCAL BUCKLING OF PULTRUDED GFRP I-SECTION COLUMNS

G. G. Cintra

D. C. T. Cardoso

giseleg.cintra@aluno.puc-rio.br

dctcardoso@puc-rio.br

Pontifical Catholic University of Rio de Janeiro

Rua Marquês de São Vicente, 225 - Gávea, 22430-060, Rio de Janeiro - RJ, Brazil

J. D. Vieira

janinedv@id.uff.br

Federal Fluminense Univesity

Av. Milton Tavares de Souza, s/n - Gragoatá, 24210-346, Niterói - RJ, Brazil

Abstract. *This paper aims to present the results of an experimental program on the local buckling behavior of GFRP I-section column. Characterization tests were made to determine the material properties and twenty-eight stub columns having three different flange-to-web ratios, overall lengths and end-condition were tested under compression. With the aid of the software GBTUL, based on the Generalized Beam Theory, the so-called signature curves (critical stress versus length) were obtained and lengths were determined to ensure 'pure' local buckling. Experimental data are reported and a discussion on the observed behavior is made, including strength, pre-buckling behavior, post-buckling reserve of strength and the influence of length and end-conditions in the critical load. It is also shown that the use of traditional Southwell plot technique leads to greater critical loads.*

Keywords: *Glass fiber reinforced polymer (GFRP); local buckling; column; end-condition*

1. INTRODUCTION

Glass-fiber reinforced polymers (GFRP) have contributed to advance civil engineering due to its several advantages over traditional materials, including their corrosion resistance, lightweight and versatility in section geometry and properties. The pultrusion process has reduced the manufacturing costs, increasing the quality control and becoming a fast and economical method of producing GFRP profiles. Since 1990's, the use of these structures has increased, with applications in pedestrian bridges, cooling towers, bridges decks, as well as in the rehabilitation and transformation of existing buildings.

To spread and encourage the use of the material and allow for safe structural design, considerable research has been conducted worldwide to develop standard provisions. Although modern, the preliminary versions of these documents still contain old-fashioned conservative equations for prediction of local buckling critical stress of I-section columns and, therefore, additional studies on the local buckling behavior are still necessary.

2. PREVIOUS STUDIES

Although a considerable number of researches on local buckling of I-section columns have been conducted in recent years, there still remain gaps in the understanding of these structures. Table 1 presents a summary of lengths, end-conditions and cross-section geometries (flange width-to-section depth, bf/d, ratio) adopted in previous studies. As can be noticed, the columns lengths reported in literature vary widely. The lack of consensus on the most appropriate columns' length, added to end-conditions not well defined may lead to a wide range of results and interpretations.

Table 1. Length, flange-to-depth ratio and end-conditions adopted on previous studies

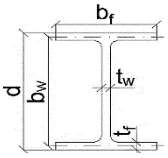		**Yoon (1993)**	**Tomblin and Barbero (1994)**	**Barbero and Trovillion (1998)**	**Pecce and Cosenza (2000)**	**Turvey and Zhang (2006)**	**Cardoso et al. (2015)**	**Present Study**
Lengths		892-3048	267-1003	1511-1816	500	200-800	152-400	300-600
End-condition	**CC** (1)			x				x
	SS (2)							x
	CB (3)	x	x		x	x	x	x
b_f/d	**0.5**						x	x
	0.75						x	x
	1.0	x	x	x	x	x	x	x

(1) Plates clamped at both ends

(2) Plates simply supported at both ends

(3) Plates simply in contact with base plates at both ends

Most of the authors performed tests with the parallel ends of the columns simply in contact with the universal testing machine base plates (CB). This configuration restrains the constituent plates rotations, but does not reproduce a clamped end-condition (CC). Additionally, local buckling is related to plate bending and therefore, the end-conditions of the constituent plates may affect significantly the results. Only Barbero and Trovillion (1998) adopted a set-up materializing clamped end-conditions for the constituent plates.

Furthermore, with exception of Cardoso *et al.* (2015), all mentioned previous works focused on I-sections having flange width equal to their depth ($b_f/d = 1.0$). Local buckling of these 'square' I-sections is governed by flange properties, in special by the shear modulus (G_{LT}). In this case, buckling is characterized by large deflections, once the critical loads (F_{crl}) are much lower than material strength (F_c). Therefore, these sections allow better and easier test monitoring. However, it is important to increase the available data on sections with different flange-to-depth ratios.

In order to obtain the experimental local buckling critical loads, Southwell plot (Southwell, 1932) was adopted in most works. This traditional method consists in linearizing the hyperbolic curve P *versus* displacements δ (or w) in a δ *versus* δ/P curve. The critical load P_{cr} is obtained as the slope of the linear portion of the plot. However, according to Bazant and Cedolin (2010), this technique is not the most appropriate for structures with post critical reserve of carrying capacity, such as plates. This behavior results in a stiffening of the system, associated with nonlinear strain distributions throughout cross-section. Furthermore, the post-critical path of a plate is completely different from the hyperbolic relationship predicted by Southwell plot, affecting its linearity. Therefore, this method may overestimate the actual critical loads. This has been discussed by Spence and Walker (1975) and Barbero and Trovillion (1998), which proposed alternative methods in order to take into account this 'stiffening' effect.

3. INFLUENCE OF LENGTH AND END-CONDITION ON P_{CR}

The influence of length and end-conditions on the local buckling critical load (P_{cr}) can be analyzed by the signature curve. This is unique for each structural member and provide the 'distance' between global (GB) and local buckling (LB). Signature curve can be obtained analytically or by using numerical methods such as the Generalized Beam Theory (GBT) (Schardt, 1994). GBT has been widely used to investigate the buckling behavior of cold-formed steel members. Schardt (1994) derived an equation where plate element contribution is considered within beam geometric stiffness. To do so, buckling mode is decomposed into a linear combination of cross-section deformation modes, offering the possibility to obtain the contribution of each one into the final buckling mode (Camotim and Basaglia, 2013).

Figure 1 presents an illustrative signature curve obtained with the GBT-based software GBTul 2.0 (Bebiano *et al.*, 2008) for an I-section column (101.6 x 101.6 x 6.4-mm). It can be noticed that length and end-conditions have strong influence on the critical load P_{cr}. The local buckling (solid lines) is associated with plate flexure and therefore, it depends on the *plates* flexural properties and end-conditions (clamped - CC or simply supported – SS at both ends). On the other hand, global buckling curves (dashed lines) are influenced by compressive modulus and *columns* boundary-conditions (pinned – PP or fixed – FF at both ends). Stubs with clamped plates tend to exhibit greater critical loads than those with simply-supported edges.

Nevertheless, as columns length increase, the end-conditions influence reduces and LB critical loads become similar for columns with both CC and SS plates.

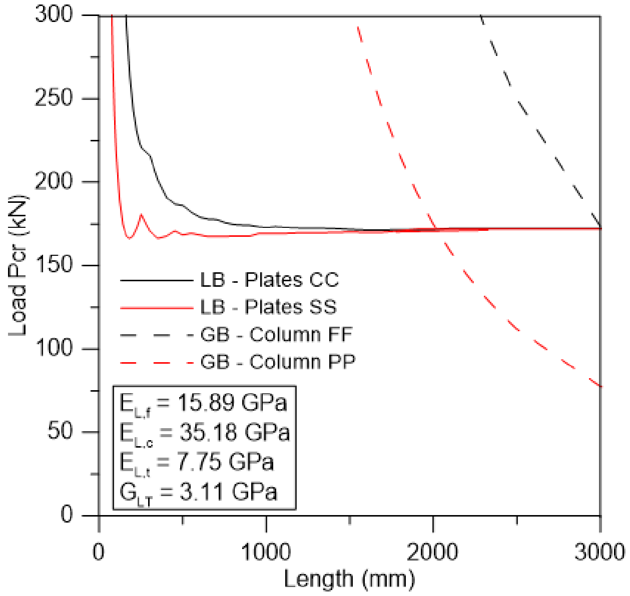

Figure 1. Signature curve: Length *versus* Critical loads

For this reason, the choice of column length is one of the most important issues to be addressed on a local buckling test. If it is desirable to mitigate the influence of boundary conditions on the tests, greater lengths should be selected. However, in these cases, interaction between LB and GB buckling may occur, reducing significantly the capacity and affecting the member behavior (Barbero and Tomblin, 1994). As shown in Figure 1, GB critical loads are lower for pin-ended columns (PP) than for fixed-ended ones (FF), and the latter must be preferred to avoid interaction.

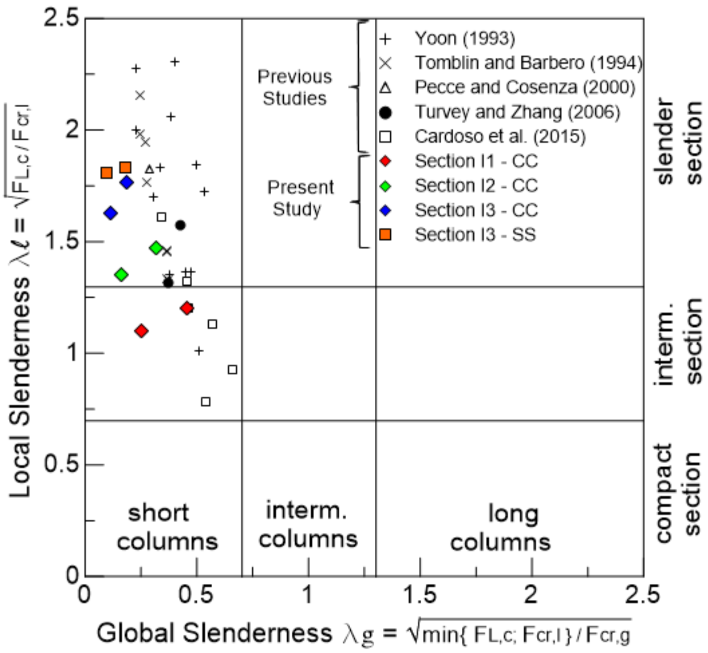

Figure 2. Local *versus* global slenderness map

Proceedings of the XXXVIII Iberian Latin-American Congress on Computational Methods in Engineering
P.O. Faria, R.H. Lopez, L.F.F. Miguel, W.J.S. Gomes, M. Noronha (Editores), ABMEC, Florianópolis, SC, Brazil, November 5-8, 2017.

Finally, interaction between LB and crushing may also occur. A local *versus* global slenderness map method was proposed by Cardoso *et al.* (2014) in order to ensure the appropriate distance between the possible failure modes. The map constitutes an important tool to provide columns classification and expected failure modes. This prediction is based on the combination of local and global non-dimensional slenderness defined on the map (λ_l and λ_g). As can be observed, to ensure 'pure' LB, the columns must be relatively short with slender sections. Figure 2 presents the map with data reported both on previous and present study. As can be observed, most of tested columns fit in the region governed by local buckling failure mode.

4. EXPERIMENTAL PROGRAM

Twenty-eight GFRP I-section stubs, made with E-glass fibers were tested. Three different cross sections geometries with distinct resins were studied: I_1) 152.4 x 76.2 x 9.5-mm (b_f/d = 0.5) having polyester resin (PO); I_2) 101.6 x 76.2 x 6.4-mm (b_f/d = 0.75) having vinylester resin (ES); and I_3) 101.6 x 101.6 x 6.4-mm (b_f/d = 1.0) having vinylester resin (ES). With the aid of the software GBTul 2.0, theoretical critical loads were predicted and appropriate lengths were determined in order to ensure 'pure' local buckling.

4.1. Material Characterization

Relevant materials properties, presented in Table 2, were determined experimentally for a better agreement with theory. Non-standard tests were particularly adopted when determining transverse properties, once the coupons could not be extracted with dimensions required in standards. Characterization tests are presented in Figure 3.

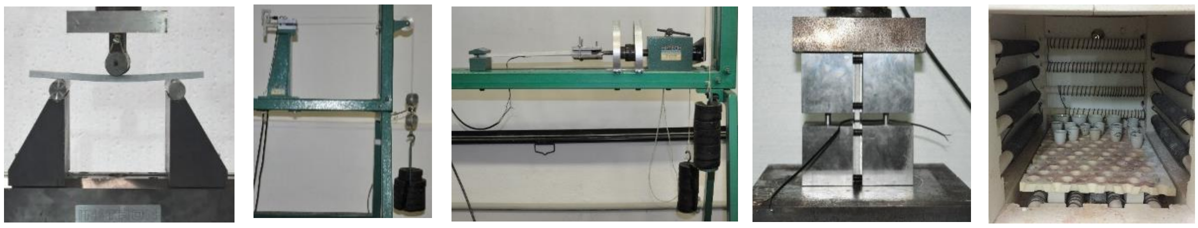

(a) (b) (c) (d) (e)

Figure 3. Material characterization tests: (a) three-point longitudinal bending test; (b) transverse bending test; (c) torsion test; (d) CLC test; (e) burn out test

Table 2. Characterization tests and properties obtained

Properties	I_1	I_2 / I_3
Longitudinal bending modulus $E_{L,f}$ (GPa)	14.73 ± 3.33	15.89 ± 1.76
Transverse bending modulus $E_{T,f}$ (GPa)	5.84	7.75
Shear modulus G_{LT} (GPa)	2.26	3.11
Longitudinal compressive modulus $E_{L,c}$ (GPa)	24.27 ± 4.38	33.70 ± 1.75
Fiber volume ratio V_f (%)	32.81± 4.19	39.94 ± 3.29

4.2. Stub Columns Tests

In the tests, the columns bases were fixed at both ends (FF), *i.e.*, overall rotation restrained. Whereas three different end-conditions, shown in Figure 4, were considered for the *plates edges*: clamped (CC), simply-supported (SS) and simply in contact with end base plates (CB) at both ends. Two different lengths were selected for each cross-section and end-condition: 300 and 600 mm for I_1; 250 and 550 mm for I_2; 300 and 550 mm for I_3 sections. Tests were conducted at a rate of 0.6 mm/min until failure. The columns were instrumented with three displacements transducers at the point where maximum out-of-plane deflections were expected, according to GBTul.

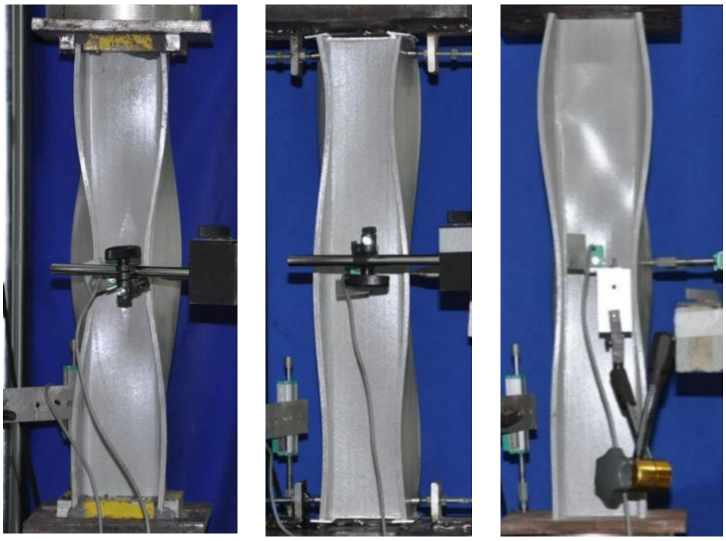

(a) (b) (c)

Figure 4. Three analyzed plates end-conditions: (a) clamped (CC); (b) simply-supported (SS); (c) simply in contact with bases (CB)

4.2.1. Columns with clamped edges

Eighteen stubs with clamped edges were tested and the behavior of columns with different flange-to-depth ratio b_f/d, overall lengths were analyzed. In order to avoid rotation of constituent plates, steel plates were attached with screws to the base plates, forming an I-shape.

A plastic filler material was applied between the base and the profiles, as shown in Figure 5 to uniform loading throughout the cross-section.

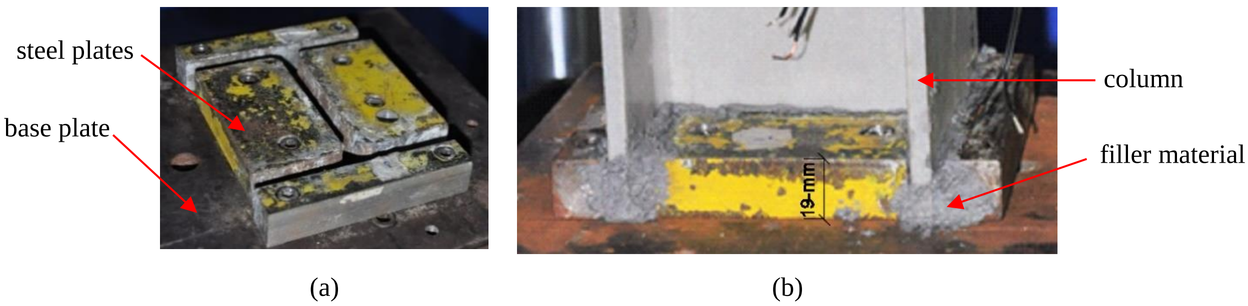

Figure 5. Set-up for columns with clamped edges: (a) steel plates attached to base plates; (b) clamped edges

Figure 6 presents P *versus* δ curves for shorter and longer columns, with the experimental results for each section and displacement transducer. As can be noticed, I_1 sections ($b_f/d=0.5$) reached the highest strengths, without a pronounced post-critical path. Little out-of-plane deflections were observed before an extremely brittle failure. This is probably due to interaction between crushing and local buckling failure modes, in accordance with the slenderness map, presented in Figure 2. On the other hand, I_3 sections ($b_f/d=1.0$) presented the largest displacements and a well-marked post-critical path, with a notable post-buckling reserve of strength. I_2 sections ($b_f/d=0.75$) constituted an intermediary case.

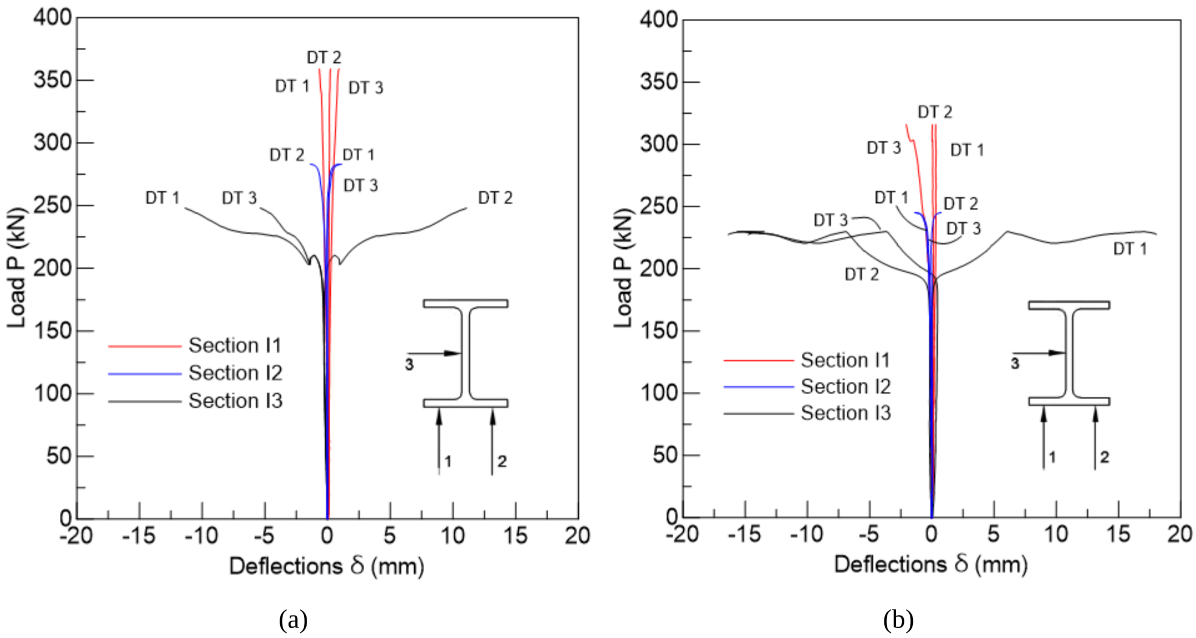

Figure 6. Experimental results: a) P *versus* δ curves for shorter stubs; b) P *versus* δ curves for longer stubs

Table 3. Comparison between experimental and theoretical critical loads (CC edges)

	Stubs	L (mm)	Experimental P_{cr} ($P_{cr.exp}$)	Theoretical P_{cr} ($P_{cr.theo}$)	$P_{cr.exp}/P_{cr.theo}$
I_1 Section (b_f/d=0.5)	01	300	386.61	476.40	0.81
	02		399.95		0.84
	03		486.11		1.02
	04	600	369.47	395.30	0.93
	05		374.39		0.95
	06		411.42		1.04
I_2 Section (b_f/d=0.75)	07	250	271.00	261.00	1.04
	08		264.40		1.01
	09		271.05		1.04
	10	550	239.22	218.95	1.09
	11		254.68		1.16
	12		258.57		1.18
I_3 Section (b_f/d=1.0)	13	300	213.27	210.20	1.01
	14		222.74		1.01
	15		227.56		1.08
	16	550	195.78	178.30	1.10
	17		204.58		1.15
	18		202.22		1.13

The experimental critical loads were obtained by Southwell plot and compared with theoretical predictions, as shown in Table 3. As can be observed, I_1 sections presented the highest differences, reaching 19%. This may be explained by the little deflections captured by the displacement transducers, leading to certain inaccuracy on Southwell plot. The results may also have been affected by damages in the material associated to the elevated applied loads. For I_2 and I_3 sections, all experimental results were greater than the theoretical ones, with differences lower than 8% for shorter stubs and up to 18% for longer columns. The higher differences observed may be due to the stiffening effect, provided by strains distributions throughout cross-section. This effect seems to be more pronounced in longer columns. Despite these differences, results seem to be in good agreement with theory.

4.2.2. Columns with simply-supported edges

One of the major challenges of this work was the reproduction of a boundary condition as close as possible to an ideal column with simply-supported edges. To allow the edges to rotate, but with translation restrained, rollers were welded to base plates and used to support the columns. Suitable results were reached when using a 2-mm steel I-sheets between the roller and the columns, avoiding end-crushing, as shown in Figure 7. Little cuts were introduced on sheets corners to reduce torsional stiffness and allow them to follow columns edges rotation. However, this set-up could not be applied on I_1 and I_2 sections, once they exhibited end crushing due to nonlinear stresses distribution through thickness. In all, six I_3 profiles having lengths equal to 300 and 550 mm were tested.

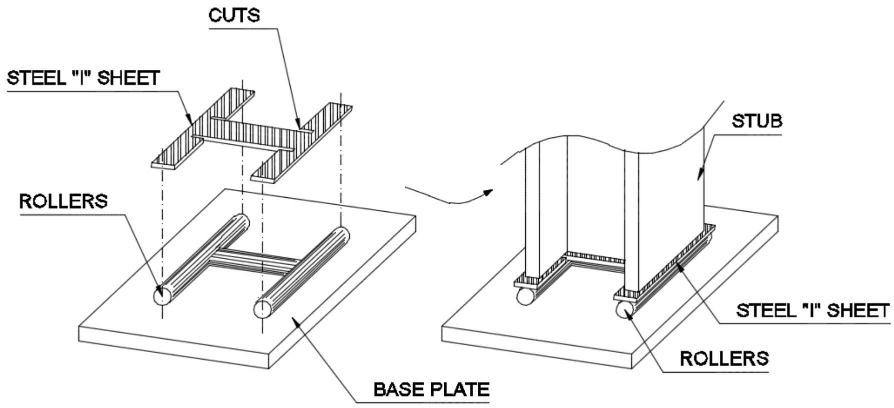

Figure 7. Set-up for columns with simply supported edges

Table 4. Comparison between experimental and theoretical critical loads (SS edges)

Stubs	L (mm)	Experimental P_{cr} ($P_{cr.exp}$)	Theoretical P_{cr} ($P_{cr.\ theo}$)	$P_{cr.exp}/P_{cr.theo}$
01		191.78		1.11
02	300	202.07	172.02	1.17
03		202.56		1.18
04		180.81		1.07
05	550	171.63	168.51	1.02
06		181.50		1.08

Table 4 presents the comparison between experimental critical loads obtained by Southwell plot and theoretical predictions obtained by GBTUL. The average differences registered were 15.3 % for shorter columns and 5.6 % for longer ones. The greater differences observed may be due to the torsional stiffness provided by the steel plate used in the test-fixture, which seems to be more pronounced in the shorter columns.

4.2.3. Columns simply in contact with base plates

For comparison purposes, four I_3 profiles were tested under the same end-conditions adopted by other authors: columns having the edges simply in contact with base plates (CB). In these conducted tests, it was evident that the base plates restrained the rotation of the plates, as shown in Figure 8. It can be noticed that there is a loss of contact between a part of the wall and the base plate. This leads to a shift in the reaction force that causes a restoring eccentricity that reduces the deflections, thus increasing the experimental critical loads (Cardoso *et al.*, 2015).

Figure 8. End of an I_3 stub tested on a direct contact condition

Figure 9 presents the theoretical signature curves for clamped and simply supported columns, as well as the experimental results for the three studied boundary conditions. It can be observed that most results for CB columns are much closer to theoretical and experimental critical loads for CC plates. The ratio of experimental results of CB columns and theoretical predictions for CC columns were lower than 4% for shorter stubs and 14% for longer ones. On the other hand, differences of 27% were found for theoretical predictions of shorter SS columns and 21% for longer ones. It can be observed that differences between the results for CC and SS end-conditions reduce as the number of half-waves increases. A suggestion for future works is to test longer columns fitting in the slenderness region governed by local buckling, but with lengths corresponding to 4,5 or more half-wavelengths, in such a way that the end-conditions be irrelevant.

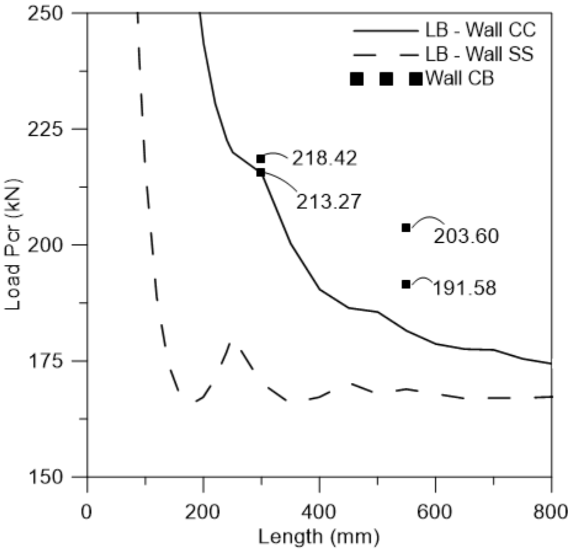

Figure 9. Theoretical signature curves and experimental results for I_3 stubs

5. CONCLUSION

A review on the previous researches exclusively dedicated to I-section local buckling columns was presented, as well as the discussion about the use of Southwell plot on thin-walled structures. Additionally, an experimental program on pGFRP I-section columns, having different flange-to-depth ratio (b_f/d), overall lengths and end-conditions were reported. The following conclusions are drawn from this study:

1. the signature curve and the local *versus* global slenderness map were presented as important tools in order to conduct a successful buckling test, providing theoretical critical loads and expected failure modes. It is important to point out that the signature curve must be obtained using adequate materials properties and, in experimental programs, experimentally determined properties must be used.
2. the test set-up for clamped plates worked well, with negligible rotation at the ends. Interaction between global and local buckling modes was observed in I_1 sections ($b_f/d=0.5$), which experienced very little deflections followed by very sudden failure. On the other hand, the slender sections I_3 ($b_f/d=1.0$) presented notable post-buckling reserve of strength and greater deflections, resulting on a stiffening of the system that may explain the greater differences observed between experimental and theoretical critical loads;
3. The adopted method to determine the experimental critical loads (Southwell plot) is not perfectly linear, leading to a possible range of different results.
4. Although the difficulties in reproducing simply-supported plates end-conditions, good results were achieved, presenting experimental critical loads closer from theoretical predictions than the ones of columns with edges simply in contact with base plates.
5. The set-up for SS columns edges apparently worked well, allowing plates rotation, although a torsional stiffening provided by the steel plates might have resulted in higher experimental critical loads.

ACKNOWLEDGEMENTS

The first author acknowledges CAPES for the financial support. In addition, the authors would like to thank the Brazilian company Cogumelo for manufacturing and supplying all pultruded GFRP used in this investigation.

REFERENCES

Barbero, Ever J., & Trovillion, J. “Prediction and measurement of the post-critical behavior of fiber-reinforced composite columns.” *Composites science and technology* 58.8 (1998): 1335-1341.

Barbero, E. J., & DeVivo, L. “Beam-column design equations for wide-flange pultruded structural shapes.” *Journal of Composites for Construction* 3.4 (1999): 185-191.

Bazant, Z. P., & Cedolin, L. “*Stability of structures: elastic, inelastic, fracture and damage theories*.” *World Scientific, Sigapore* (2010).

Bebiano, R., Pina, P., Silvestre, N., and Camotim, D. (2008). GBTUL – buckling and vibration analysis of thin-walled members. DECivil/IST, Technical University of Lisbon, Lisbon (http://www.civil.ist.utl.pt/gbt).

Camotim, D., & Basaglia, C. (2013). Buckling Analysis of thin-walled steel structures using generalized beam theory (GBT): state-of-the-art report. *Steel Construction*, 6(2), 117-131

Cardoso, Daniel C.T., Harries, Kent A. & Batista, E. M. “Compressive strength equation for GFRP square tube columns." *Composites Part B: Engineering* 59 (2014): 1-11.

Cardoso, Daniel C. T., Harries, Kent A. & Batista, E. M. "Compressive local buckling of pultruded GFRP I-sections: development and numerical/experimental evaluation of an explicit equation." *Journal of Composites for Construction* 19.2 (2015): 04014042.

Pecce, M., and Cosenza, E. "Local buckling curves for the design of FRP profiles." *Thin-walled structures* 37.3 (2000): 207-222.

Schardt, R. "Generalized beam theory - an adequate method for coupled stability problems." *Thin-Walled Structures* 19.2-4 (1994): 161-180.

Spencer, H. H., and A. C. Walker. "Critique of Southwell plots with proposals for alternative methods." *Experimental Mechanics* 15.8 (1975): 303-310.

Southwell, Richard V. "On the analysis of experimental observations in problems of elastic stability." *Proceedings of the Royal Society of London A: Mathematical, Physical and Engineering Sciences*. Vol. 135. No. 828. The Royal Society, 1932.

Turvey, G. J., and Zhang, Y. "A computational and experimental analysis of the buckling, postbuckling and initial failure of pultruded GRP columns." *Computers & structures* 84.22 (2006): 1527-1537.

Yoon, S. J. *Local buckling of pultruded I-shape columns*. Diss. Georgia Institute of Technology, 1993.